Inorg. Chem. **2004**, *43*, 6215–6223

Synthesis, Characterization, and Detailed Electrochemistry of Binuclear Ruthenium(III) Complexes Bridged by Bisacetylacetonate. Crystal and Molecular Structures of [{Ru(acac)$_2$}$_2$(tae)] (acac = 2,4-Pentanedionate Ion, tae = 1,1,2,2-Tetraacetylethanate Dianion)

Tomohiro Koiwa,[†] Yuki Masuda,[†] Junpei Shono,[†] Yuji Kawamoto,[†] Yoshimasa Hoshino,[‡] Takeshi Hashimoto,[†] Karuppannan Natarajan,[§] and Kunio Shimizu*,[†]

Department of Chemistry, Faculty of Science and Technology, Sophia University, 7-1 Kioicho, Chiyoda-ku, Tokyo 102-8554, Japan, Department of Chemistry, Faculty of Education, Nagasaki University, 1-14 Bunkyo-machi, Nagasaki 852-8521, Japan, and Department of Chemistry, Bharathiar University, Coimbatore 641046, India

Received July 3, 2003

Binuclear β-diketonatoruthenium(III) complexes [{Ru(acac)$_2$}$_2$(tae)], [{Ru(phpa)$_2$}$_2$(tae)], and [(acac)$_2$Ru(tae)-Ru(phpa)$_2$] and binuclear and mononuclear bipyridine complexes [{Ru(bpy)$_2$}$_2$(tae)](PF$_6$)$_2$ and [Ru(bpy)$_2$(Htae)]PF$_6$ (acac = 2,4-pentanedionate ion, phpa = 2,2,6,6-tetramethyl-3,5-heptanedionate ion, tae = 1,1,2,2-tetraacetylethanate dianion, and bpy = 2,2′-bipyridine) were synthesized. The new complexes have been characterized by ^{1}H NMR, MS, and electronic spectral data. Crystal and molecular structures of [{Ru(acac)$_2$}$_2$(tae)] have been solved by single-crystal X-ray diffraction studies. Crystal data for the meso isomer of [{Ru(acac)$_2$}$_2$(tae)] have been confirmed by the dihedral angle result that two acetylacetone units of the bridging tae ligand are almost perpendicular to one another. A detailed investigation on the electrochemistry of the binuclear complexes has been carried out. The electrochemical behavior details of the binuclear complexes have been compared with those of the mononuclear complexes obtained from the half-structures of the corresponding binuclear complexes. Studies on the effects of solvents on the mixed-valence states of Ru^{II}–Ru^{III} and Ru^{III}–Ru^{IV} complexes have been carried out by various voltammetric and electrospectroscopic techniques. A correlation between the comproportionation constant (K_c) and the donor number of the solvent has been obtained. The K_c values for the binuclear complexes have been found to be low because of the fact that two acetylacetone units of the bridging tae ligand are not in the same plane, as revealed by the crystal structure of [{Ru(acac)$_2$}$_2$(tae)].

Introduction

Mixed-valence materials that contain an element in more than one oxidation state have attracted chemists for many years. Binuclear ruthenium complexes form, by far, the largest group of such systems. Robin and Day's class II and class III types of such mixed-valence complexes of ruthenium have been reviewed.[1] In general, ligand-bridged binuclear mixed-valence complexes provide convenient systems for modeling inter- and/or intramolecular electron transfer and related processes.[2] Pentaammineruthenium derivatives of these types of complexes have been extensively studied and reviewed.[1,3] Polynuclear ruthenium complexes of polypyridyl ligands are also currently being investigated for applications

* Author to whom correspondence should be addressed. E-mail: simizu-k@sophia.ac.jp.
[†] Sophia University.
[‡] Nagasaki University.
[§] Bharathiar University.

(1) Crutchley, R. J. *Adv. Inorg. Chem.* **1994**, *41*, 273.

(2) Meyer, T. J. *Acc. Chem. Res.* **1978**, *11*, 94. (b) *Mixed-Valence Compounds: Theory and Applications in Chemistry, Physics, Geology, and Biology*, Proceedings of the NATO Advanced Study Institute, Oxford, England, Sept 10−21, 1979; Brown, D. B., Ed.; Reidel Publishing: Dordrecht, The Netherlands, 1980. (c) Newton, M. D.; Sutin, N. *Annu. Rev. Phys. Chem.* **1984**, *35*, 437. (d) Newton, M. D. *Chem. Rev.* **1991**, *91*, 767. (e) *Electron Transfer in Inorganic, Organic, and Biological Systems*; Bolton, J. R., Mataga, N., McLendon, G., Eds.; Advances in Chemistry Series 228; American Chemical Society: Washington, DC, 1991. (f) *Electron Transfer Reactions: Inorganic, Organometallic and Biological Applications*; Isied, S. S., Ed.; Advances in Chemistry Series 253; American Chemical Society: Washington, DC, 1997. (g) Brunschwig, B. S.; Sutin, N. *Coord. Chem. Rev.* **1999**, *187*, 233.

10.1021/ic030216c CCC: $27.50
Published on Web 09/03/2004

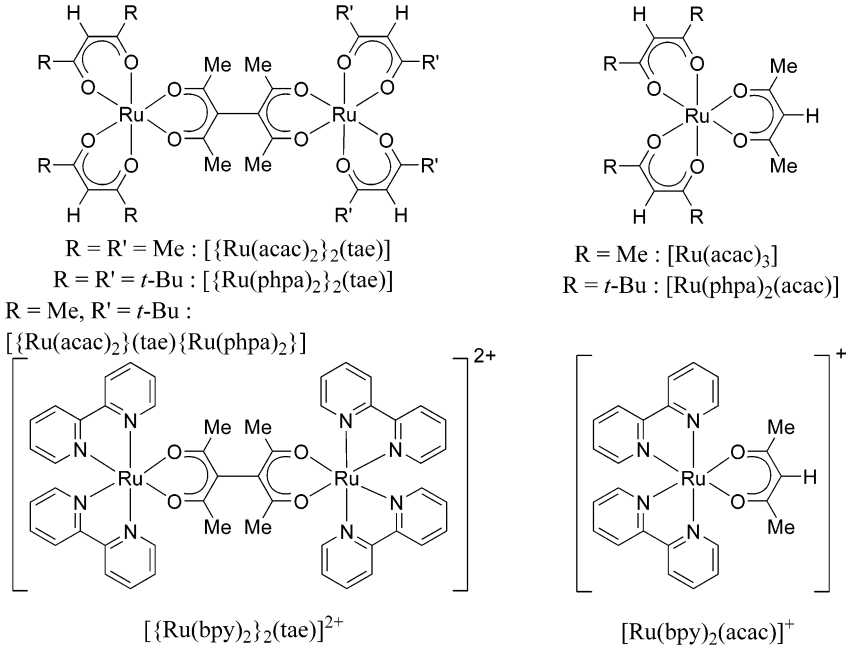

Figure 1. Structures of the binuclear complexes bridged with bisacetylacetonate dianion and of the mononuclear complexes obtained from exactly half structures of the corresponding binuclear complexes.

in various supramolecular structures as electronic and photomolecular devices.[4] The nature of the bridging ligands is the key component in these systems. In fact, the size, shape, and electronic nature of the bridging ligands control the electronic communication between two metal centers in such binuclear complexes. In this regard, many polyaromatic compounds have been used as bridges between two metal centers.[5] Though many aromatic systems have been used as bridging ligands in binuclear ruthenium complexes, little attention has been paid to nonaromatic bridging ligands.[6] The authors have already reported the binuclear complexes, $[\{Ru(acac)_2\}_2(L)]$, in which two $\{Ru(acac)_2\}$ moieties were bridged with aromatic[7] and nonaromatic[8] compounds. Recently, a binuclear complex, $[\{Ru(acac)_2\}_2(L)]$, in which the bridging ligand L^{2-} contains a $^{-}HN-C{=}N-N{=}C-NH^{-}$ unit arising from the two-electron reduction of the 1,4-dihydro-1,2,4,5-tetrazine component of H_2L, has been reported.[9] The comproportionation constants (K_cs) of the binuclear complex were much larger than those of the binuclear complexes bridged with tae because of the better ability of the bridging ligand to delocalize electrons. It will be interesting to study the effects of the change of terminal ligands and the change of length of the bridging ligands on the electron delocalization between the metal ions in binuclear complexes. In this connection, β-diketonato derivatives of ruthenium are excellent systems. One can have five possible combinations of oxidation states ($Ru^{II}-Ru^{II}$, $Ru^{II}-Ru^{III}$, $Ru^{III}-Ru^{III}$, $Ru^{III}-Ru^{IV}$, and $Ru^{IV}-Ru^{IV}$) in the binuclear complexes, enabling one to study the mixed-valence states. To observe the mixed-valence states and to see the effect of changing terminal ligands in controlling the redox potentials of binuclear ruthenium complexes, we have carried out systematic investigations on the reactions of $[Ru(acac)_2(AN)_2]PF_6$ (AN = CH_3CN), $[Ru(phpa)_2(AN)_2]PF_6$, and $[Ru(bpy)_2Cl_2]Cl{\cdot}2H_2O$ with bis(acetylacetone) (H_2tae). In this paper, we report the synthesis, characterization, and detailed electrochemical investigations of tae^{2-}-bridged binuclear ruthenium complexes.

Results and Discussion

Synthesis and Characterization. The general structures of the binuclear complexes and the mononuclear complexes, which are exactly one-half of the structure of the corresponding binuclear complexes, are given in Figure 1.

(3) Creutz, C. *Prog. Inorg. Chem.* **1983**, *30*, 1. (b) Ward, M. D. *Chem. Soc. Rev.* **1995**, *34*, 121.
(4) Balzani, V.; Juris, A.; Venturi, M.; Campagna, S.; Serroni, S. *Chem. Rev.* **1996**, *96*, 759−834. (b) Venturi, M.; Serroni, S.; Juris, A.; Campagna, S.; Balzani, V. T. *Top. Curr. Chem.* **1998**, *197*, 193. (c) Besler, P.; Bernhard, S.; Blum, S.; Beyeler, A.; De Cola, L.; Balzani, V. *Coord. Chem. Rev.* **1999**, *155*, 190. (d) Barigelletti, F.; Flamigni, L. *Chem. Soc. Rev.* **2000**, *29*, 1.
(5) Bogler, J.; Gourdon, A.; Ishow, E.; Launay, J. P. *J. Chem. Soc., Chem. Commun.* **1995**, 1799. (b) Bogler, J.; Gourdon, A.; Ishow, E.; Launay, J. P. *Inorg. Chem.* **1996**, *35*, 2937. (c) MacDonnell, F. M.; Bodige, S. *Inorg. Chem.* **1996**, *35*, 5758. (d) Bodige, S.; Torres, A. S.; Maloney, D. J.; Tate, D.; Kinsel, G. R.; Walker, A. K.; MacDonnell, F. M. *J. Am. Chem. Soc.* **1997**, *119*, 10364. (e) Barigelletti, F.; Flamigni, L.; Collin, J. P.; Sauvage, J. P. *Chem. Commun.* **1997**, 333. (f) Campagna, S.; Serroni, S.; Bodige, S.; MacDonnell, F. M. *Inorg. Chem.* **1999**, *38*, 692. (g) MacDonnell, F. M.; Kim, M. J.; Bodige, S. *Coord. Chem. Rev.* **1999**, *535*, 185. (h) Ali, M.; McDonnell, F. M. *J. Am. Chem. Soc.* **2000**, *122*, 11527.
(6) Ward, M. S.; Chatterjee, D.; Shepherd, R. E. *Polyhedron* **2000**, *19*, 1339. (b) Patra, S.; Mondal, B.; Sarkar, B.; Niemeyer, M.; Lahiri, G. K. *Inorg. Chem.* **2003**, *42*, 1322. (c) Tinnemans, A. H. A.; Timmer, K.; Reinten, M.; Kraaijkamp, J. G.; Alberts, A. H.; Van Der Linden, J. G. M.; Schmitz, J. E. J.; Saaman, A. A. *Inorg. Chem.* **1981**, *20*, 3698.
(7) Hashimoto, T.; Endo, A.; Nagao, N.; Satô, G. P.; Natarajan, K.; Shimizu, K. *Inorg. Chem.* **1998**, *37*, 5211.
(8) Kasahara, Y.; Hoshino, Y.; Kajitani, M.; Shimizu, K.; Satô, G. P. *Organometallics* **1992**, *11*, 1968. (b) Hoshino, Y. *Platinum Met. Rev.* **2001**, *45*, 2.
(9) Patra, S.; Miller, T. A.; Sarkar, B.; Niemeyer, M.; Ward, M. D.; Lahiri, G. K. *Inorg. Chem.* **2003**, *42*, 4707.

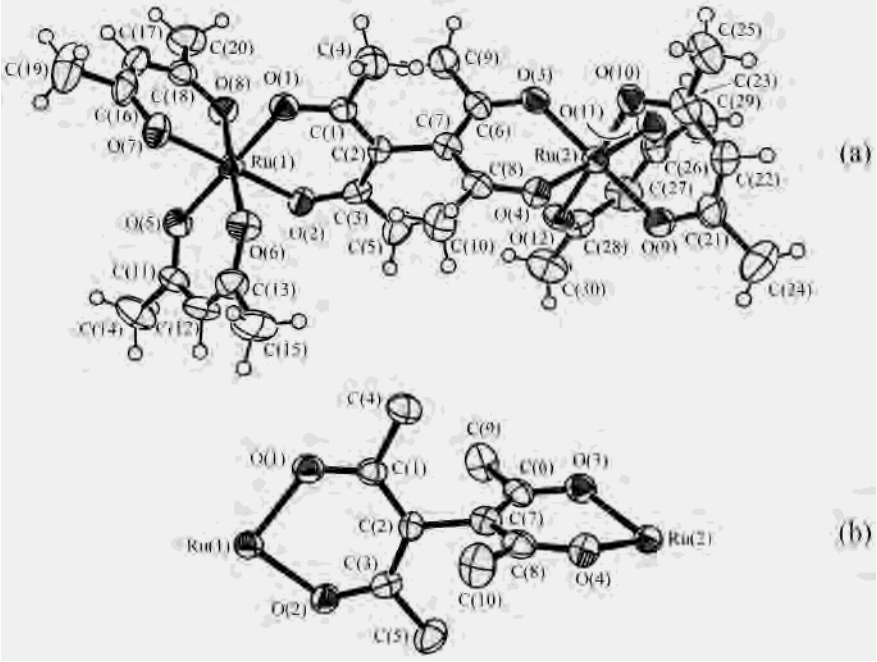

Figure 2. ORTEP diagram of the meso isomer of [{Ru(acac)$_2$}$_2$(tae)] with an atomic labeling scheme (a) and the skeleton (b) showing the two acetylacetonato groups of the bridging ligand, which are perpendicular to one another.

The reaction of [Ru(acac)$_2$(AN)$_2$]PF$_6$ with H$_2$tae in toluene solution gave two isomers of [{Ru(acac)$_2$}$_2$(tae)] (**1**), which were labeled **1a** (the first fraction in chromatography) and **1b** (the second one). For such a binuclear complex, there are theoretically two diastereomers, racemic ($\Delta-\Delta$ and $\Lambda-\Lambda$) and meso ($\Delta-\Lambda$), and two fractions are found. When this reaction is carried out with [Ru^{II}(acac)$_2$(AN)$_2$] instead of [Ru^{III}(acac)$_2$(AN)$_2$]PF$_6$, complex **1** is also obtained with less yield. Additionally, mononuclear [Ru(acac)$_2$(Htae)] was also obtained by these reactions.

Isomers **1a** and **1b** gave identical FAB-MS spectra with a parent ion peak ($m^+/z = 796$); their ^{1}H NMR spectra looked very similar, with the characteristic paramagnetic shift due to the Ru^{III} that was present in the complexes.

Analysis of the X-ray crystal structure (to be discussed later) showed that **1a** was the meso ($\Delta-\Lambda$) isomer, and hence **1b** should be the racemic isomer (the mixture of $\Delta-\Delta$ and $\Lambda-\Lambda$).

Since [Ru^{II}(phpa)$_2$(AN)$_2$] was unstable, the reaction of H$_2$tae with [Ru^{III}(phpa)$_2$(AN)$_2$]PF$_6$ was carried out; this gave, in addition to binuclear [{Ru(phpa)$_2$}$_2$(tae)] (**2**), mononuclear complex [Ru(phpa)$_2$(Htae)]. The TLC of the binuclear complex showed two very close spots, which could not be further separated. This indicates that complex **2** is a mixture of meso and racemic isomers, as described in binuclear complex **1**. The elemental analysis of the mixture corresponded to complex **2**. Its IR spectrum showed a band at 2962 cm^{-1}, which is characteristic of the C−H stretching frequency of the *tert*-butyl group. Complex **2** was also obtained from the reaction between [Ru(phpa)$_2$(Htae)] and [Ru(phpa)$_2$(AN)$_2$]PF$_6$.

The reaction of [Ru(acac)$_2$(Htae)] and [Ru(phpa)$_2$-(AN)$_2$]PF$_6$ yielded two isomers, which correspond to mixtures of the meso ($\Lambda-\Delta$ and $\Delta-\Lambda$) and racemic ($\Delta-\Delta$ and $\Lambda-\Lambda$) isomers of [(acac)$_2$Ru(tae)Ru(phpa)$_2$] (**3**). The two types of isomers were named **3a** (the first fraction in chromatography**)** and **3b** (the second one).

Table 1. Crystal Data and Structure Refinement for [{Ru(acac)$_2$}$_2$(tae)] (Meso)

empirical formula	$Ru_2C_{30}H_{40}O_{12}$
fw	794.78
cryst syst	monoclinic
space group	$P2_1/c$
unit-cell dimensions	
a (Å)	8.248(4)
b (Å)	17.015(7)
c (Å)	24.613(11)
β (deg)	92.642(5)
Z	4
V (Å)	3450.5(26)
ρ calcd (g cm^{-3})	1.530
μ (cm^{-1})	9.32
R_1[a]	0.083
R_w[b]	0.157

[a] $R_1 = \sum||F_o| - |F_c||/\sum|F_o|$. [b] $R_w = [\sum(w(F_o^2 - F_c^2)^2)/\sum w(F_o^2)^2]^{1/2}$.

Structure of [{Ru(acac)$_2$}$_2$(tae)] (1a). The crystal of complex **1a** contains four molecules in the unit cell. From the ORTEP diagram shown in Figure 2, complex **1a** was found to be the meso isomer. Crystal data and structure refinements are listed in Table 1, and important bond lengths and bond angles are given in Table 2. The bond lengths and bond angles found for the terminal acetylacetonato groups are similar to those observed for [Ru(acac)$_3$].[10] However, some significant differences have been seen in the acetylacetonato groups of the bridging ligand. One set of the diagonally opposite Ru−O bonds of the bridging ligand shows a bond length of 1.98 Å, while the other set shows a slightly longer bond length of 2.00 Å. The terminal Ru−O bonds show a uniform length of 2.00 Å. The C−O distances

(10) Chao, G. K. J.; Sime, R. L.; Sime, R. J. *Acta Crystallogr.* **1973**, *B29*, 2845.

Table 2. Major Interatomic Distances (Å) and Interatomic Angles (deg) for [{Ru(acac)$_2$}$_2$(tae)] (Meso)

Ru(1)−O(1)	2.001(5)	O(1)−Ru(1)−O(2)	91.6(2)
Ru(1)−O(2)	1.987(5)	O(1)−Ru(1)−O(6)	87.7(2)
Ru(1)−O(5)	2.012(5)	O(1)−Ru(1)−O(7)	88.8(2)
Ru(1)−O(6)	2.002(5)	O(1)−Ru(1)−O(8)	91.3(2)
Ru(1)−O(7)	2.008(5)	O(2)−Ru(1)−O(6)	88.6(2)
Ru(1)−O(8)	2.009(5)	O(2)−Ru(1)−O(8)	88.4(2)
Ru(2)−O(3)	1.980(5)	O(5)−Ru(1)−O(6)	92.5(2)
Ru(2)−O(4)	2.009(5)	O(5)−Ru(1)−O(7)	89.8(2)
Ru(2)−O(9)	2.003(5)	O(5)−Ru(1)−O(8)	88.6(2)
Ru(2)−O(10)	2.029(5)	O(6)−Ru(1)−O(7)	90.5(2)
Ru(2)−O(11)	2.007(5)	O(1)−Ru(1)−O(5)	178.6(2)
Ru(2)−O(12)	2.008(5)	O(2)−Ru(1)−O(7)	179.0(2)
O(1)−C(1)	1.281(9)	O(6)−Ru(1)−O(8)	176.8(2)
O(2)−C(3)	1.299(9)	O(3)−Ru(2)−O(9)	176.2(2)
O(3)−C(6)	1.291(9)	O(4)−Ru(2)−O(11)	177.9(2)
O(4)−C(8)	1.289(9)	O(10)−Ru(2)−O(12)	177.2(2)
O(5)−C(11)	1.29(1)	O(3)−Ru(2)−O(4)	89.6(2)
O(6)−C(13)	1.29(1)	O(3)−Ru(2)−O(10)	90.2(2)
O(7)−C(16)	1.28(1)	O(3)−Ru(2)−O(11)	89.2(2)
O(8)−C(18)	1.284(9)	O(3)−Ru(2)−O(12)	89.3(2)
O(9)−C(21)	1.30(1)	O(4)−Ru(2)−O(9)	93.4(2)
O(10)−C(23)	1.27(1)	O(4)−Ru(2)−O(10)	89.9(2)
O(11)−C(26)	1.26(1)	O(9)−Ru(2)−O(10)	92.2(2)
O(12)−C(28)	1.28(1)	O(9)−Ru(2)−O(11)	87.9(2)

of the bridging ligand (1.28−1.30 Å) show slightly higher values than those found for the terminal acetylacetonato units (1.26−1.28 Å). This trend has been seen in the C−C distances, as well. However, the C−CH$_3$ bonds of the bridging ligand and of the terminal ligands show the same length of 1.50 Å. The dihedral angle between the two planes consisting of O(1)−C(1)−C(2)−C(3)−O(3) and O(3)−C(6)−C(7)−C(8)−O(4) has been found to be 94°, indicating that the two acetylacetonato groups of the bridging ligand are almost perpendicular to one another. This is expected, not only due to the free rotation of the two rings through the C−C bond but also due to the steric repulsions from the four methyl groups. The O−Ru−O bond angles are normal at ∼90°, as expected for the coordinated acetylacetonate. The nonbonding Ru−Ru distance is 8.05 Å, which is the length of the bridging ligand.

^{1}H NMR Spectra. The ^{1}H NMR spectral data and the assignments are given in the Experimental Section. The chemical shifts for all of the complexes, except [Ru(bpy)$_2$(acac)]$^+$ and [{Ru(bpy)$_2$}$_2$(tae)]$^{2+}$, have been observed over a wide range from 4.28 to −48.55 ppm. This is characteristic of the paramagnetic shift due to the presence of ruthenium(III), which is a d^5 system with one unpaired electron. There are many factors, apart from electron density, which affect the chemical shifts of these systems. Especially in the case of mixed-ligand complexes, both metal−ligand and ligand−ligand interactions have to be considered. The paramagnetic shifts in all of the ruthenium(III) complexes can arise from both the contact interaction and the pseudocontact interaction.[11] All of the methine proton signals have been shifted to locations upfield from the corresponding signals of the diamagnetic ruthenium(II) complexes.[12] There were three signals due to the three different methyl groups present in complexes **1a** and **1b**, but the precise assignment could not be made. Hence, from the ^{1}H NMR spectra, the isomers could not be identified. The ^{1}H NMR spectra of both mixtures of isomers (**1** and **2**) were similar.

[Ru(bpy)$_2$(acac)]PF$_6$ and [{Ru(bpy)$_2$}$_2$(tae)](PF$_6$)$_2$ (**4**) showed normal chemical shifts for the protons present as they are in diamagnetic ruthenium(II) complexes. Dimeric complex **4** showed two singlets at 1.56 and 1.58 ppm for the methyl groups due to the presence of two isomers. The signal due to bipyridine appeared as a multiplet from 7.32 to 8.72 ppm. Monomeric complex [Ru(bpy)$_2$(acac)]PF$_6$ showed a singlet at 1.83 ppm for the methyl group, another singlet at 5.32 ppm for the proton of the γ-carbon atom, and a multiplet from 7.09 to 8.66 ppm for the bipyridine group.

Table 3. Electronic Spectral Data of Binuclear and Related Mononuclear Complexes in Acetonitrile

complexes	λ_{max}, nm (ϵ, mol^{-1} m^2)
[{Ru(acac)$_2$}$_2$(tae)] (meso)	273 (3.35), 358 (3.07), 516 (2.41)
[{Ru(acac)$_2$}$_2$(tae)] (racemic)	273 (3.47), 359 (3.23), 516 (2.56)
[{Ru(phpa)$_2$}$_2$(tae)]	276 (3.60), 367 (3.30), 516 (2.64)
[{Ru(bpy)$_2$}$_2$(tae)](PF$_6$)$_2$	246 (3.68), 289 (3.91), 295 (3.96), 374 (3.37), 514 (3.20), 554 (3.08)
[Ru(acac)$_3$]	272 (3.24), 349 (2.94), 506 (2.19)
[Ru(phpa)$_2$(acac)]	276 (3.31), 357 (2.96), 500 (2.30)
[Ru(bpy)$_2$(acac)](PF$_6$)	294 (3.50), 369 (2.80), 513 (2.72), 562 (2.54)

Electronic Spectra. The electronic spectra data of the complexes in acetonitrile solution are presented in Table 3. All of the new β-diketonato complexes showed three bands in the region from 273 to 516 nm. The spectra of the dinuclear β-diketonato complexes are very similar to that observed for [Ru(acac)$_3$]. However, molar absorption coefficients (ϵ) of all of the bands for the binuclear β-diketonato complexes are higher than that found for [Ru(acac)$_3$]. UV−vis spectra of some tris(β-diketonato)ruthenium(III) complexes have been assigned.[6] Kobayashi et al. ascribed the three absorption bands of [Ru(acac)$_3$] to the excited states which were the configuration-interaction admixture of the ligand-to-metal charge-transfer (LMCT) excited states and to the ligand ($\pi-\pi^*$) excited triplets and singlets.[13] The three absorption spectra of the binuclear β-diketonato complexes can be assigned as in the case of [Ru(acac)$_3$]. Hence, the bands observed in the regions of 516−525 and 273−276 nm could be assigned to the triplet and singlet $\pi-\pi^*$ charge transfer, respectively. However, the bands around 360 nm are assigned to the metal-to-ligand charge-transfer (MLCT) bands. It is to be pointed out here that these assignments fit very well with the assignments made for [Ru(acac)$_3$].

Among the six bands of the electronic spectrum of bipyridine complex [{Ru(bpy)$_2$}$_2$(tae)](PF$_6$)$_2$, three bands at 554, 514, and 374 nm were similar to those observed for the binuclear complexes of the {Ru(bpy)$_2$} unit that was bridged by various bridging ligands. Hence, on the basis of the positions of the bands and the molar absorption coefficients, the bands observed at 554 and 514 nm are attributed to the MLCT of Ru^{II}−bpy (π^*).[14] The higher-energy band observed at 374 nm has been assigned to the bpy $\pi-\pi^*$

(11) Eaton, D. R. *J. Am. Chem. Soc.* **1965**, *87*, 3097.
(12) Palmer, R. A.; Fay, R. C.; Piper, T. S. *Inorg. Chem.* **1964**, *3*, 875. (b) Holm, R. H.; Cotton, F. A. *J. Am. Chem. Soc.* **1958**, *80*, 5658. (c) Fay, R. C.; Piper, T. S. *J. Am. Chem. Soc.* **1963**, *85*, 500.
(13) Kobayashi, H.; Matsuzawa, H.; Kaizu, Y.; Ichida, A. *Inorg. Chem.* **1987**, *26*, 4318.

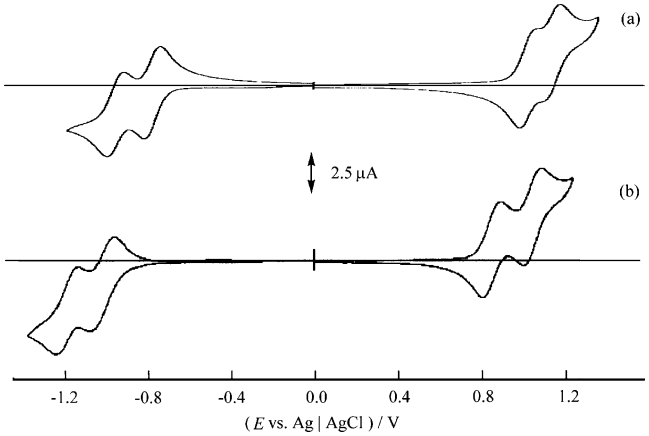

Figure 3. Cyclic voltammograms of $[\{Ru(acac)_2\}_2(tae)]$ (a) and $[\{Ru(phpa)_2\}_2(tae)]$ (b) in 0.1 mol dm^{-3} tetraethylammonium perchlorate/acetonitrile solutions at 25 °C. The concentration of the complex = 1 mmol dm^{-3}, and the potential scan rate = 0.1 V s^{-1}.

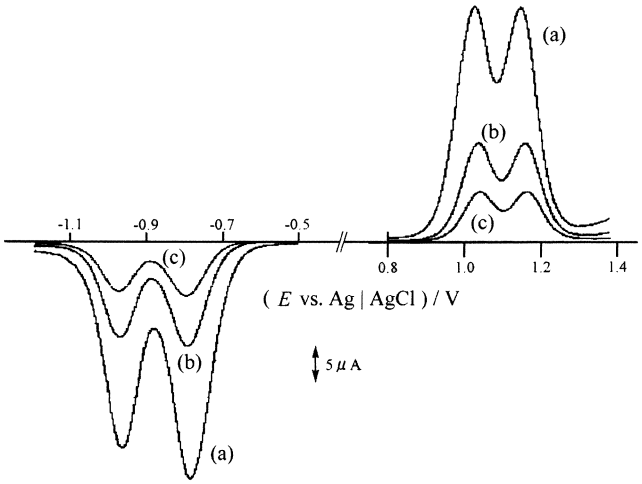

Figure 4. Typical differential pulse voltammograms for complex $[\{Ru(acac)_2\}_2(tae)]$ in 0.1 mol dm^{-3} tetraethylammonium perchlorate/acetonitrile solutions at 25 °C. The concentration of the complex = 1 mmol dm^{-3}; the potential scan rate = 2 mV s^{-1}, and the pulse amplitude (ΔE) = (a) 50, (b) 20, or (c) 10 mV.

charge transition. The electronic spectrum of $[Ru(bpy)_2(acac)]PF_6$ showed bands at 562, 513, 369, and 294 nm. Here again, on the basis of the assignments made above, the bands observed from 513 to 562 nm are attributed to the MLCT of $Ru^{II}-bpy$ (π^*), and the other high-energy bands at 369 and 294 nm are assigned to the charge-transfer transitions of the $\pi-\pi^*$ (bpy) charge transfer.

Electrochemistry. Typical cyclic and differential pulse voltammograms of complex **1** (mixture of **1a** and **1b**) and complex **2** in a dichloromethane medium are shown in Figures 3 and 4, respectively. Two pairs of peaks on both the positive and the negative potential sides of the cyclic voltammogram correspond to two consecutive and Nernstian one-electron oxidation ($Ru^{III}-Ru^{III} \rightarrow Ru^{III}-Ru^{IV} \rightarrow Ru^{IV}-Ru^{IV}$) and reduction ($Ru^{III}-Ru^{III} \rightarrow Ru^{II}-Ru^{III} \rightarrow Ru^{II}-Ru^{II}$) steps. The differential pulse voltammograms also showed two peaks on each side, corresponding to the two pairs of peaks observed in the cyclic voltammograms. The reversible half-wave potentials ($E_{1/2}$) of the binuclear and the related mononuclear complexes in acetonitrile solutions are given in Table 4. The $E_{1/2}$ values for complex **2** have been shifted toward more negative values compared to those of complex **1**, which is an indication of more electron donation by the terminal *tert*-butyl group than by the methyl group. This is clearly reflected in the very small negative shift in the half-wave potential of complex **2** compared to the shift for $[Ru(phpa)_3]$. In the heterobinuclear complex, $[(acac)_2Ru(tae)Ru(phpa)_2]$, the first oxidation and reduction $E_{1/2}$ values correspond to those of the $\{Ru(phpa)_2\}$ and $\{Ru(acac)_2\}$ moieties, respectively.

The cyclic voltammogram of the bipyridine binuclear complex, $[\{Ru(bpy)_2\}_2(tae)](PF_6)_2$ (**4**), in acetonitrile solution showed two peaks for the stepwise oxidations from $Ru^{II}-Ru^{II}$ to $Ru^{II}-Ru^{III}$ and $Ru^{III}-Ru^{III}$. However, the separation between the two oxidation potentials is very small compared to that found for complexes **1** and **2**. This indicates that the presence of a mixed-valence state of $Ru^{II}-Ru^{III}$ in binuclear complex **4** is not as stable as in complexes **1** and **2**.

The equilibrium constants (K_c) for the comproportionation reaction in the binuclear systems are defined as

$$\text{Oxidation: } Ru^{III}-Ru^{III} \underset{E_{1/2}(ox1)}{\overset{-e^-}{\rightleftharpoons}} Ru^{III}-Ru^{IV} \underset{E_{1/2}(ox2)}{\overset{-e^-}{\rightleftharpoons}} Ru^{IV}-Ru^{IV}$$

$$\text{Reduction: } Ru^{III}-Ru^{III} \underset{E_{1/2}(red1)}{\overset{e^-}{\rightleftharpoons}} Ru^{II}-Ru^{III} \underset{E_{1/2}(red2)}{\overset{e^-}{\rightleftharpoons}} Ru^{II}-Ru^{II}$$

$$K_c(III-IV) = \frac{[Ru^{III}-Ru^{IV}]^2}{[Ru^{III}-Ru^{III}][Ru^{IV}-Ru^{IV}]}$$

$$K_c(II-III) = \frac{[Ru^{II}-Ru^{III}]^2}{[Ru^{III}-Ru^{III}][Ru^{II}-Ru^{II}]}$$

$$K_c = \exp\left(\frac{F}{RT}\left|E_{1/2}(1) - E_{1/2}(2)\right|\right)$$

Here, $E_{1/2}(1)$ and $E_{1/2}(2)$ are the reversible half-wave potentials corresponding to $Ru^{III}-Ru^{III}/Ru^{III}-Ru^{IV}$ (or $Ru^{III}-Ru^{III}/Ru^{II}-Ru^{III}$) and $Ru^{III}-Ru^{IV}/Ru^{IV}-Ru^{IV}$ (or $Ru^{II}-Ru^{III}/Ru^{II}-Ru^{II}$), respectively. Cyclic voltammograms of complex $[\{Ru(acac)_2\}_2(tae)]$ in different organic solvents are shown in Figure 5. The log K_c(II−III) and log K_c(III−IV) values with each $E_{1/2}$ for binuclear complexes **1** and **2** found in different solvents are given in Table 4. Both of the log K_c values for phpa complex **2** have been found to be higher than those found for acac complex **1**. This may be due to the *tert*-butyl groups in each phpa donating more electrons to the ruthenium ion, resulting in higher values for log K_c(II−III) and log K_c(III−IV). Besides, the log K_c values for the mixed-valence states ($Ru^{II}-Ru^{III}$) are higher than those found for $Ru^{III}-Ru^{IV}$, irrespective of the solvents used. This is true for both complex **1** and complex **2**, with only one exception. However, a low value of log K_c (1.42) for

(14) Bolger, J.; Gourdon, A.; Ishow, E.; Launay, J. P. *Inorg. Chem.* **1996**, *35*, 2937. (b) Ishow, E.; Gourdon, A.; Launay, J. P.; Chiorboli, C.; Scandola, F. *Inorg. Chem.* **1999**, *38*, 1504.

Table 4. Half-Wave Potentials ($E_{1/2}$) of Binuclear and Related Mononuclear Complexes and Comproportionation Constants (K_c) of Binuclear Complexes in Various Organic Solvents

solvents (donor number)	complexes	$E_{1/2}$ (vs Fc/Fc^+) (V)				log K_c	
		red2	red1	ox1	ox2	$Ru^{II}-Ru^{III}$	$Ru^{III}-Ru^{IV}$
acetonitrile (14.1)	$[\{Ru(acac)_2\}_2(tae)]$	−1.32	−1.18	0.57	0.68	2.3	1.8
	$[\{Ru(phpa)_2\}_2(tae)]$	−1.48	−1.33	0.47	0.60	2.5	2.2
	$[\{Ru(acac)_2\}(tae)\{Ru(phpa)_2\}]$	−1.56	−1.29	0.50	0.69	4.5	3.1
	$[\{Ru(bpy)_2\}_2(tae)](PF_6)_2$			0.20	0.29	1.4	
	$[Ru(acac)_3]$		−1.16	0.60			
	$[Ru(phpa)_2(acac)]$		−1.35	0.49			
	$[Ru(bpy)_2(acac)](PF_6)$			0.21			
dichloromethane (0)	$[\{Ru(acac)_2\}_2(tae)]$	−1.49	−1.31	0.53	0.65	3.0	2.0
	$[\{Ru(phpa)_2\}_2(tae)]$	−1.73	−1.55	0.34	0.54	3.0	3.4
benzonitrile (11.9)	$[\{Ru(acac)_2\}_2(tae)]$	−1.44	−1.28	0.54	0.65	2.7	1.9
	$[\{Ru(phpa)_2\}_2(tae)]$	−1.58	−1.41	0.43	0.57	2.9	2.4
dimethylformamide (26.6)	$[\{Ru(acac)_2\}_2(tae)]$	−1.38	−1.22	0.56	0.66	2.7	1.7
	$[\{Ru(phpa)_2\}_2(tae)]$	−1.54	−1.37	0.47	0.59	2.9	2.0

binuclear bipyridine complex **4** in acetonitrile solution has been observed, which indicates that the mixed-valence state ($Ru^{II}-Ru^{III}$) in this complex is not as stable as that found for β-diketonato complexes **1** and **2**. The log K_c values of the complexes have been plotted against the donor number of the solvents used; the result is given in Figure 6. From the plot, it is clear that the log K_c values are higher for solvents with low donor numbers. For example, dichloromethane, with a lower donor value, shows higher log K_c values when compared with the lower values shown by the higher donor solvent acetonitrile. A recent study showed that the potential required to form a charged mixed-valence complex varied markedly depending on the nature of the electrolyte used.[15] When the solvent effect for K_c is discussed, the electrolyte effects also need to be considered.

The electronic spectral changes of binuclear acac complexes **1** and **2** during controlled potential oxidations and reductions were measured using an optically transparent thin-layer electrochemical electrode (OTTLE) cell. It is observed from the spectra that all of the five possible combinations of oxidation states ($Ru^{II}-Ru^{II}$, $Ru^{II}-Ru^{III}$, $Ru^{III}-Ru^{III}$, $Ru^{III}-Ru^{IV}$, and $Ru^{IV}-Ru^{IV}$) were found to be stable for complex **2** and all but one ($Ru^{IV}-Ru^{IV}$) were stable in the case of complex **1**. A typical electronic spectral change during the reduction is shown in Figure 7. From the spectra, it is clear that the spectrum of a binuclear complex after one electron reduction ($Ru^{III}-Ru^{III}$ to $Ru^{II}-Ru^{III}$) is almost the same as that obtained for a mixture of mononuclear complexes of Ru(III) and Ru(II). This is indicative of the existence of mixed-valence states in the binuclear complexes. As expected, a similar behavior has been noticed in the case of oxidations, too. During the reduction, a peak around 520 nm has appeared in the electronic spectra of both complex **1**

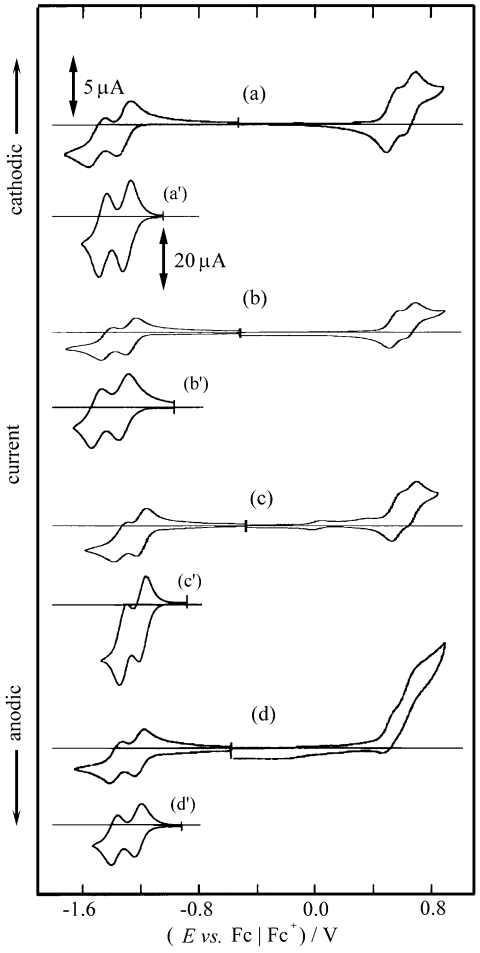

Figure 5. Cyclic voltammograms of complex $[\{Ru(acac)_2\}_2(tae)]$ in 0.1 mol dm^{-3} tetraethylammonium perchlorate − different organic solvents at 25 °C. Potential scan rate was 0.1 V s^{-1} (a) in dichloromethane, (b) in acetonitrile, (c) in benzonitrile, and (d) in dimethylformamide. The reduction side of cyclic voltammograms (a′−d′) was obtained using the OTTLE cell.

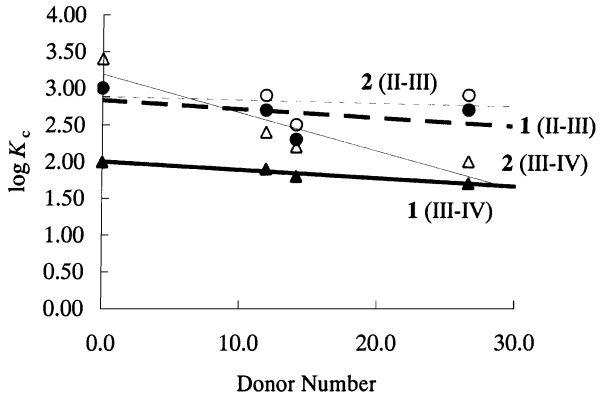

Figure 6. Plots of log K_c(II−III) and log K_c(III−IV) in 0.1 mol dm^{-3} tetrabutylammonium perchlorate against the donor number of the solvents for binuclear complexes $[\{Ru(acac)_2\}_2(tae)]$ (**1**) and $[\{Ru(phpa)_2\}_2(tae)]$ (**2**) at 25 °C. The straight lines represent the lines fitted by least-squares.

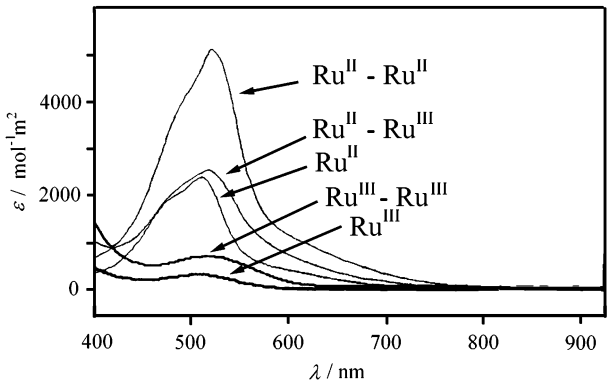

Figure 7. Comparison of electronic spectra of the ruthenium(III) and ruthenium(II) complexes in 0.1 mol dm^{-3} tetraethylammonium perchlorate/acetonitrile solutions. $Ru^{III}-Ru^{III}$, $[\{Ru(acac)_2\}_2(tae)]$; $Ru^{II}-Ru^{III}$, $[\{Ru(acac)_2\}_2(tae)]^-$; $Ru^{II}-Ru^{II}$, $[\{Ru(acac)_2\}_2(tae)]^{2-}$; Ru^{III}, $[Ru(acac)_3]$; and Ru^{II}, $[Ru(acac)_3]^-$.

and complex **2**. However, no peak could be observed for complex **1** during oxidation, even though a peak at 700 nm could be seen during oxidation for complex **2**. This is due to the fact that the two oxidations are too close to one another, as has already been seen when the cyclic voltammogram of complex **1** was compared to that of complex **2**. It is to be noted that the normal electronic spectral behavior of complex **1** is almost identical to that of complex **2**.

The near-infrared spectra corresponding to the intervalence electron transfer of the one-electron oxidation and reduction of both complexes **1** and **2** were sought by using an OTTLE cell in the range of 800−2400 nm, but no significant spectra could be obtained because of the very small molar absorption coefficients of these mixed-valence complexes.

Conclusion

Three types of binuclear β-diketonatoruthenium complexes (**1**−**3**) and a bipyridineruthenium complex (**4**), bridged with a bisacetylacetonate ion, were prepared. Binuclear complex **1** separated into meso and racemic isomers. The configuration of the meso isomer showed that the two acetylacetonatoruthenium rings of the bridging ligand were almost perpendicular to one another. Such a structure of the binuclear β-diketonato and bipyridine complexes weakened the electron interaction between the two ruthenium atoms, and this was reflected in the K_c values. The K_c value of the binuclear bipyridine complex (**4**) was slightly smaller than those of the β-diketonato complexes (**1** and **2**). From the electrochemical studies, it is concluded that binuclear complexes **1**, **2**, and **4** fall into class II of the Robin and Day classification.

Both of the K_c(II−III) and K_c(III−IV) values of the phpa binuclear complex (**2**) were larger than those of the acac binuclear complex (**1**). This would be due to the electrodonating properties of the *tert*-butyl groups in the phpa ligand. Furthermore, it was found that the K_c(II−III) values were larger than those of the K_c(III−IV) in both acac and phpa complexes, as shown in Table 4. Thus, the magnitudes of K_c(II−III) and K_c(III−IV) were reversed in the case of the binuclear complex bridging by HN−C═N−N═C−NH.[9]

Experimental Section

Physical Measurements. ^1H NMR spectra were recorded in $CDCl_3$ with a JEOL GX-270 spectrophotometer ($SiMe_4$ as the internal reference). UV−vis spectra were recorded on a Hitachi model U-3210 spectrometer. IR spectra were recorded with a JIR-3001 FT-IR spectrophotometer and EI- and FAB-MS spectra with a JEOL JMS-D300 or JMS-SX102A spectrometer.

X-ray Crystallography. Crystal data and structure determination parameters are given in Table 1. Single crystals of complex **1a**, suitable for diffraction studies, were grown by the vapor diffusion of *n*-hexane into a solution of the complex in chloroform. Single crystal data collections were performed at 298 K with a Rigaku AFC8 Mercury-CCD diffractometer using graphite monochromated Mo Kα (λ = 0.7170 Å) radiation. The data were collected and processed using the CrystalClear software package of Rigaku Corp.[16] The structure was solved by direct methods[17] and was expanded using Fourier techniques.[18] For all of the complexes, Empirical absorption corrections were applied using Lorentz polarization and absorption. The non-hydrogen atoms were refined anisotropically. All hydrogen atoms were refined using the riding model. All calculations were performed using the CrystalStructure[19] crystallographic software package.

Voltammetric Analysis. The voltammetric equipment used here has been described previously.[7] A suitable OTTLE cell, which was fabricated in this laboratory, has been used for in situ measurement of the visible absorption spectra during electrolysis.[20] The effective light path length of the OTTLE cell was ∼0.3 mm, and the effective volume was 60 mm^3. Spectral measurements for the OTTLE cell were made using a spectro-multichannel photodetector (Photal MCPD-1000) with a personal computer (NEC PC-9801VX) attached to a plotter (Photal MC-920). All of the potentials were measured against Ag/AgCl (3 mol dm^{-3} aqueous NaCl solution). The average potential of the reference electrode at 25 °C was −0.52 V (in dichloromethane and benzonitrile), −0.47 V (in acetonitrile), and −0.58 V (in dimethylformamide) against the half-wave potential of the Fc/Fc^+ couple. The reference electrode was connected to the test solution through a 0.1 mol dm^{-3} tetrabutylammonium perchlorate (TBAP) solution with a Vycor plug filled with the background solution. A platinum disk with a diameter of 1.6 mm embedded in Teflon was used as the test electrode for the cyclic, the normal pulse, and the differential pulse voltammetric experiments. A spiral platinum wire was used as the auxiliary electrode.

The reversible half-wave potentials, $E_{1/2}$, were determined from the peak potential of the cyclic voltammogram or the normal pulse voltammogram by means of the conventional logarithmic plot method in a Nernstian case. In cases where two waves overlap, $E_{1/2}$ was determined from the peak of the differential pulse

(15) Barrière, F.; Camire, N.; Geiger, W. E.; Mueller-Westerhoff, U. T.; Sanders, R. *J. Am. Chem. Soc.* **2002**, *124*, 7262.

(16) (a) *CrystalClear*; Rigaku Corporation, 1999. (b) *CrystalClear Software User's Guide*; Molecular Structure Corporation: Olem, UT, 2000. (c) Pflugrath, J. W. *Acta Crystallogr.* **1999**, *D55*, 1718.

(17) Altomare, A.; Cascarano, G.; Giacovazzo, C.; Guagliardi, A.; Burla, M.; Polidori, G.; Camalli, M. *J. Appl. Crystallogr.* **1994**, *27*, 435.

(18) Beurskens, P. T.; Admiraal, G.; Beurskens, G.; Bosman, W. P.; de Gelder, R.; Israel, R.; Smith, J. M. M. *DIRDIF99*; Technical Report of the Crystallography Laboratory, University of Nijmegen: Nijmegen, The Netherlands, 1999.

(19) *CrystalStructure Analysis Package*; Rigaku and Rigaku/MSC: The Woodlands, TX, 2000−2003. (b) Watkin, D. J.; Prout, C. K.; Carruthers, J. R.; Betteridge, P. W. *Crystals Issue 10*; Chemical Crystallography Laboratory: Oxford, England, 1996.

(20) Endo, A.; Mochida, I.; Shimizu, K.; Satô, G. P. *Anal. Sci. Jpn.* **1989**, *62*, 709.

voltammogram.[21] In quasi-reversible cases, $E_{1/2}$ was approximated by $(E_{pa} + E_{pc})/2$, where E_{pa} and E_{pc} are the potentials of the anodic and the cathodic peaks of the cyclic voltammogram, respectively.

Materials. Acetonitrile, dichloromethane, and dimethylformamide were purchased from Wakojunyaku Kogyo Corp. and were dried by 3 and 4 Å molecular sieves purchased from the same company. Benzonitrile was purchased from Tokyo Kasei Corp. and was dried by 3 and 4 Å molecular sieves. Spectroscopic-grade acetonitrile from Dojin Laboratories was used for spectroscopic work. The supporting electrolyte, TBAP (special polarographic grade), was purchased from Nakarai Chemicals, Ltd. For synthetic experiments, commercially available reagent-grade solvents and chemicals were used.

Synthesis of H_2tae (1,1,2,2-Tetraacetylethane). Na(acac) was prepared by using a modified procedure as described hereunder, and the same method was used for the preparation of H_2tae.[22] NaOH (40 g) was dissolved in 250 cm^3 of water−ethanol (1:4), and then acetylacetone (100 g) was added. When the solution was stirred, a white crystalline compound appeared. The mixture was kept in the refrigerator for 2 h. The solid was then filtered and washed with cold methanol twice. After the compound was dried under vacuum, it was heated at 100 °C under vacuum for 2 h to remove the water of crystallization. Yield: 97 g (80%). Thirteen grams of Na(acac) was taken in a mortar and ground well. It was then transferred to a 500 cm^3 conical flask, and 150 cm^3 of diethyl ether was added. The suspension was stirred vigorously, and then 12.5 g of I_2 dissolved in 150 cm^3 of ether was added dropwise. After the completion of addition, the solution was transferred to a 500 cm^3 beaker and kept at room temperature overnight. After the natural evaporation of ether, a solid compound was obtained. After the addition of 500 cm^3 of water, the solution was kept for 1 h. It was then filtered and recrystallized from hot methanol (100 cm^3). A white crystalline solid was obtained. Yield: 1.51 g (14.3%). Anal. Calcd for $C_{10}H_{14}O_4$: C, 60.59; H, 7.12. Found: C, 60.31; H, 7.13.

Syntheses of $[Ru^{III}(acac)_2(AN)_2]PF_6$ and $[Ru^{III}(phpa)_2(AN)_2]PF_6$. Synthesis of $[Ru^{III}(acac)_2(AN)_2]PF_6$ was carried out according to the following procedures.[23] $[Ru(acac)_3]$ (400 mg, 1 mmol) was dissolved in 30 cm^3 of AN, and 10 cm^3 of a 1% H_2SO_4/AN solution was slowly added to the $[Ru(acac)_3]$ solution with stirring. The solution color changed initially from wine red to deep blue. The solution was concentrated to 3 cm^3 by evaporation of the solvent. NH_4PF_6 (0.5 g, 3 mmol) was dissolved in 5 cm^3 of cold water, and this mixture was added to the deep-blue solution. The resulting deep-blue precipitate was collected by filtration, washed with cold water and then with *n*-hexane, and dried under vacuum. Yield: 50% (0.26 g). FAB-MS (m^+/z): 382 (M^+), 300 ($M^+ - 2AN$). Anal. Calcd for $RuC_{14}H_{20}F_6N_2O_4P$: C, 31.95; H, 3.83; N, 5.32. Found: C, 31.64; H, 3.97; N, 5.46. $[Ru^{III}(phpa)_2(AN)_2]PF_6$ was synthesized from $[Ru(phpa)_3]$ by using the same procedures as those used in the case of $[Ru^{III}(acac)_2(AN)_2]PF_6$. Yield: 94% (1.0 g). FAB-MS (m^+/z): 550 (M^+), 468 ($M^+ - 2AN$). Anal. Calcd for $RuC_{26}H_{44}F_6N_2O_4P$: C, 44.95; H, 6.38; N, 4.03. Found: C, 44.45; H, 6.29; N, 4.24.

Syntheses of $[Ru(acac)_2(Htae)]$ and $[\{Ru(acac)_2\}_2(tae)]$ (1) (Meso Isomer (1a) and Racemic Isomer (1b)). $[Ru(acac)_2(AN)_2]PF_6$ (0.26 g, 0.5 mmol) and H_2tae (0.05 g, 0.25 mmol) were dissolved in 100 cm^3 of toluene, and then the solution was heated under reflux for 8 h. The solvent was evaporated off; the residue was dissolved in BZ (benzene)/AN (6:1) and then subjected to column chromatography on silica gel with BZ/AN (6:1). The first red fraction contained $[Ru(acac)_2(Htae)]$ (yield based on Ru: 30%). The second red fraction gave the meso isomer **1a** (14%), and the third red fraction gave the racemic isomer **1b** (14%). Analytical data for $[Ru(acac)_2(Htae)]$ follow. FAB-MS (m^+/z): 497 (M^+), 300 ($M^+ -$ Htae). Anal. Calcd for $RuC_{20}H_{27}O_8$: C, 48.38; H, 5.48. Found: C, 48.56; H, 5.82. Analytical data for **1a** and **1b** follow. FAB-MS (m^+/z) (**1a** and **1b**): 796 (M^+), 697 ($M^+ -$ acac). Anal. Calcd for $Ru_2C_{30}H_{40}O_{12}$: C, 45.34; H, 5.07. Found: (**1a**) C, 44.53; H, 5.21; (**1b**) C, 45.29; H, 5.38. ^{1}H NMR for **1a**: δ −3.33 (12H), −6.07 (12H), −9.76 (12H) (CH_3 protons of acac or tae), −29.17 (4H) (CH protons of acac). ^{1}H NMR for **1b**: δ −3.58 (12H), −6.34 (12H), −9.34 (12H) (CH_3 protons of acac or tae), −29.60 (4H) (CH protons of acac).

Syntheses of $[Ru(phpa)_2(Htae)]$ and $[\{Ru(phpa)_2\}_2(tae)]$ (2) (Mixture of Meso and Racemic Isomers). $[Ru(phpa)_2(Htae)]$ and binuclear complex **2** were synthesized from $[Ru(phpa)_2(AN)_2]PF_6$ by using the same procedures as those used in the case of the synthesis of $[\{Ru(acac)_2\}_2(tae)]$ (**1**). The meso and racemic isomers of dinuclear complex **2** could not be separated by column chromatography. Analytical data for $[Ru(phpa)_2(Htae)]$ follow. Yield: 22% (based on Ru). FAB-MS (m^+/z): 665 (M^+), 468 ($M^+ -$ Htae). Anal. Calcd for $RuC_{32}H_{51}O_8$: C, 57.81; H, 7.73. Found: C, 57.91; H, 7.91. Analytical data for **2** follow. Yield: 38%. FAB-MS (m^+/z): 1131 (M^+), 948 ($M^+ -$ phpa), 765 ($M^+ -$ 2phpa), 468 ($M^+ - Ru(phpa)_2(tae)$). Anal. Calcd for $Ru_2C_{54}H_{88}O_{12}$: C, 57.03; H, 8.03. Found: C, 57.18; H, 8.08. ^{1}H NMR: δ 2.99 (12H) (CH_3 protons of tae), 3.08 (36H), 1.73 (36H) (*t*-Bu protons of phpa), −39.47 (4H) (CH protons of phpa).

Synthesis of $[(acac)_2Ru(tae)Ru(phpa)_2]\cdot 2CH_2Cl_2$ (3) (Meso Isomer (3a) and Racemic Isomer (3b)). $[Ru(acac)_2(Htae)]$ (0.25 g, 0.5 mmol) and $[Ru(phpa)_2(AN)_2]PF_6$ (0.35 g, 0.5 mmol) were dissolved in 100 cm^3 of toluene. The solution was heated under reflux for 6 h. The solvent was evaporated off; the residue was then dissolved in DM/AN (10:1) and subjected to column chromatography on silica gel with DM/AN (10:1). The first dark-red fraction contained complex **3a**, and the second dark-red fraction gave complex **3b**.

Analytical data for **3a** and **3b** follow. Yield: (**3a**) 10%, (**3b**) 10% (based on Ru). FAB-MS (m^+/z): 964 (M^+), 864 ($M^+ -$ acac), 665 ($M^+ - Ru(acac)_2$), 468 ($M^+ - Ru(acac)_2(tae)$). Anal. Calcd for $Ru_2C_{44}H_{68}O_{12}Cl_4$ (**3**): C, 46.65; H, 6.05. Found: C, 46.47; H, 6.06. ^{1}H NMR for **3a**: δ 4.28 (6H), −2.99 (6H), −5.96 (6H), −10.70 (6H) (CH_3 protons of acac and tae), 3.19 (18H), 1.72 (18H) (*t*-Bu protons of phpa), −28.72 (2H) (CH protons of acac), −40.86 (2H) (CH protons of phpa). ^{1}H NMR for **3b**: δ 3.77 (6H), −3.10 (6H), −6.13 (6H), −10.63 (6H) (CH_3 protons of acac and tae), 3.19 (18H), 1.72 (18H) (*t*-Bu protons of phpa), −28.72 (2H) (CH protons of acac), −40.19 (2H) (CH protons of phpa).

Synthesis of $[\{Ru(bpy)_2\}_2(tae)](PF_6)_2$ (4) (Mixture of Meso and Racemic Isomers). $[RuCl_2(bpy)_2]Cl\cdot 2H_2O$ (0.34 g, 2 mmol) was dissolved in a 1:2 water/ethanol mixture (150 cm^3); this mixture was heated to 60 °C. After H_2tae (0.13 g, 1 mmol) was added, the solution was heated under reflux for 5 min. The color of the solution changed from reddish yellow to reddish purple. After the solution was cooled to room temperature, $KHCO_3$ (0.07 g) was added and the solution was again heated under reflux for 15 min. Then the solvent ethanol was removed, and the aqueous solution was transferred to an ion-exchange column (SP-Sephadex-25). On elution with a 0.05 mol dm^{-3} NaCl solution, the first fraction gave $[Ru(bpy)_2(Htae)]Cl$. On elution with a 0.10 mol dm^{-3} NaCl solution, $[\{Ru(bpy)_2\}_2(tae)]Cl_2$ was obtained. Water was evaporated to concentrate the solution (∼5 cm^3), and a saturated solution of

(21) Richardson, D. E.; Taube, H. *Inorg. Chem.* **1981**, *20*, 1278.
(22) Charles, R. G. *Org. Synth.* **1963**, *4*, 869.
(23) Kasahara, Y.; Hoshino, Y.; Shimizu, K.; Satô, G. P. *Chem. Lett.* **1990**, 381.

NH_4PF_6(aq) was added, whereby a reddish-purple compound, $[\{Ru(bpy)_2\}_2(tae)](PF_6)_2$, separated out. It was filtered, washed with a small amount of cold water, and dried under vacuum. It was further washed with ether, and again dried under vacuum. A very similar treatment to that for the concentrated solution of $[Ru(bpy)_2(Htae)]Cl$ resulted in $[Ru(bpy)_2(Htae)]PF_6$. Analytical data for $[Ru(bpy)_2(Htae)]PF_6$ follow. Yield: 26%. Anal. Calcd for $RuC_{30}H_{29}O_4N_4PF_6$: C, 47.33; H, 3.84; N, 7.35. Found: C, 45.88; H, 3.58; N, 7.12. Analytical data for $Ru_2C_{50}H_{44}O_4N_8P_2F_{12}$ (**4**) follow. Yield: 19%. Anal. Calcd for $[\{Ru(bpy)_2\}_2(tae)](PF_6)_2$: C, 45.74; H, 3.38; N, 8.53. Found: C, 45.17; H, 3.22; N, 8.30. ^{1}H NMR: δ 1.58 (6H), 1.56 (6H) (CH_3 protons of tae), 7.32−8.72 (protons of bpy).

Acknowledgment. We thank Professor F. S. Howell, Department of Chemistry, Sophia University, for correcting this paper. We are also grateful to two reviewers for several helpful comments about this paper.

IC030216C